NUB-75-164-E
E-0233

Nucl. Phys. B

~~Phys. Lett. B~~
July 1975
#233

TWO PARTICLE RAPIDITY CORRELATIONS IN PROTON-NUCLEUS INTERACTIONS AT 300 GeV

G.Baroni, S.Di Liberto, F.Meddi, S.Petrera, G.Romano

Istituto di Fisica dell'Università, Roma
Istituto Nazionale di Fisica Nucleare, Sezione di Roma

M.Juric, O.Adamovic

University of Belgrade

I.Otterlund

Department of Cosmic High Energy Physics, University of Lund

G.Baumann, R.Devienne

Université de Nancy

H. Areti, J.Hebert

University of Ottawa

J.Lory, C.Meton, D.Schune, Tsai-Chü, B.Willot

L.P.N.H.E., Université Pierre et Marie Curie, Paris

J.M.Bolta, G.Rey

Instituto de Fisica Corpuscular, Facultad di Ciencias, Valencia

SUMMARY

The two-particle rapidity correlation in 300 GeV proton-nucleus interaction in nuclear emulsion shows clear evidence of short range correlations. A remarkable asymmetry between projectile and target hemisphere is found.

Several authors[1-3] have suggested that the study of multiparticle finals states in high energy hadronic interactions with nuclei can give useful information on the elementary hadron-nucleon process.

When multiparticle production occurs inside a nucleus the products of the first collision can interact again with the downstream nucleons: reasonable estimates indicate that, at energies higher than $\sim$100 GeV, this second interaction occurs before the asymptotic state is achieved.

Two-particles inclusive correlations, from several FNAL[4,5] and CERN-ISR[6,7] pp experiment, have given support to the idea of independent cluster emission in the elementary process; the same measurements in proton-nucleus interactions should provide further information about their space-time behaviour. For this purpose we have performed the analysis of two-particle inclusive correlations in proton-nucleus interactions at 300 GeV. Accurate angular measurements of all the shower tracks have been performed on a sample of 1045 inelastic interactions from a stack of Ilford K5 emulsions exposed at FNAL[8]. On a reduced sample ($\sim$ 350 events) the distributions of both the azimuthal angle (ϕ) and the azimuthal separation of each pair of tracks ($\Delta\phi = \phi_i - \phi_j$) were inspected in order to avoid that some lack of detection efficiency could affect the following definition of angular functions: no azimuthal dependence or correlation was observed.

We chose as polar angle variable

$$\eta = \eta_L - \ln\left(\gamma_c (1 + \beta_c)\right) \qquad (1)$$

where η_L is the pseudo-rapidity in the laboratory frame:

$$\eta_L = -\ln \tan \Theta_L / 2$$

and Θ_L is the polar angle of the emitted particle with respect to the incident proton; $\gamma_c = (1 - \beta_c^2)^{-1/2}$ is the Lorentz factor of the c.m.s. for pp collision with the proton target at rest (at 300 GeV $\gamma_c = 12.67$).

At this energy the shower particles are mainly pions, with a mean transverse momentum of ≈ 0.4 GeV/c. It follows that $p_{/\!/}^2 \gg p_\perp^2 \gg m_\pi^2$ for most of them, so that η_L closely approaches the laboratory rapidity

$$y_L = \frac{1}{2} \ln (E + p_{/\!/})/(E - p_{/\!/})$$

The correlation function we use is:

$$R(\eta_1, \eta_2) = \frac{\dfrac{1}{\sigma_{in}} \dfrac{d^2\sigma}{d\eta_1 d\eta_2} - \dfrac{1}{\sigma_{in}^2} \dfrac{d\sigma}{d\eta_1} \dfrac{d\sigma}{d\eta_2}}{\dfrac{1}{\sigma_{in}^2} \dfrac{d\sigma}{d\eta_1} \dfrac{d\sigma}{d\eta_2}} \qquad (2)$$

$$= \frac{N_T \, N_2(\eta_1, \eta_2)}{N_1(\eta_1) N_1(\eta_2)} - 1$$

where N_T is the total number of inelastic interactions in the sample, $N_1(\eta)$ is the number of prongs at η and $N_2(\eta_1, \eta_2)$ is the number of pairs of tracks with η_1 and η_2 values.

$R(\eta_1, \eta_2)$ is obviously symmetric about the line $\eta_1 = \eta_2$ due to its definition, but does not need to be symmetric for $\eta_1 = -\eta_2$

as it happens in p-p interactions, where it is imposed by the initial state symmetry.

Fig. 1 shows the single-particle inclusive rapidity distribution for three different classes of events; in fig. 2 the two-particle distribution is shown. The division of the complete sample into groups characterized by N_h (the number of heavy prongs, that is the evaporation particles emitted in the interaction) is suggested by the usually accepted idea that it is related to the mean number of collisions inside the nucleus. We chose the classes $N_h \leqslant 1$, $2 \leqslant N_h \leqslant 6$ and $N_h > 6$ in order to have three subsamples equally populated but still with sufficient statistics.

Fig. 3 shows the contour plots of the correlation function $R(\eta_1, \eta_2)$ for the same groups and for the complete sample of events. The constant-R lines were obtained by linear interpolation between the matrix elements build-up with the R-values and are drawn only in the regions of the (η_1, η_2) plane where the statistics allowed a good confidence. They have to be considered only for their general features.

Fig. 4 shows $R(\eta_1, \eta_2)$ as a function of the rapidity separation $\eta_2 - \eta_1$ for the same classes as in fig. 3 and for different values of η_1.

When removing from each event the particle emitted at the smallest angle (in most cases it is the ~~emitted~~ leading proton that takes away most of the energy) the R-values are always some~~thing~~what lower (by $\sim 5\%$), though compatible within the errors with the previous ones.

Our experimental results show that:

a) There is a clear evidence for attractive (i.e. positive) correlations: for each value of η_1 the correlation function shows a maximum at $\eta_2 - \eta_1 \approx 0$ (short range correlations). The low statistical accuracy in the regions with large rapidity separations does not allow to exclude some long-range correlation too.

b) Both the central value ($R(0,0) = 0.55 \pm 0.10$) and the correlation length ($\sim$ 2 rapidity units) agree very well with the p-p data[4-7] for the stars with smallest size ($N_h \leqslant 1$).

c) The correlation function is not symmetric for $\eta_1 = -\eta_2$ and shows a clear preference toward higher correlations in the proton-nucleon c.m. backward hemisphere ($\eta < 0$). It is found that the contours do not show a remarkable change in the forward hemisphere for different N_h groups, at least near the line $\eta_1 = \eta_2$, whereas $R(\eta_1, \eta_2)$ flattens in the backward hemisphere when increasing N_h. The maximum, however, always is confined about at the same position ($\eta \gtrsim -1.5$) despite both the single and the two-particles inclusive spectra (fig. 1 and 2) have a very different shape for different N_h.

It is to remark that the asymmetry is still present for events with $N_h \leqslant 1$, and R has for this class the maximum value, which is considerably higher than for p-p interactions.

We think that this asymmetry and the high value of R are the most striking results of the present analysis.

The effect cannot be due to the definition of the η variable, which is referred to the proton-hydrogen c.m.s.: it is easily seen that Fermi motion cannot explain such an asymmetry, because the variation produced on γ_c very little affects ($\lesssim$ 3%) the η definition, through the logarithmic transformation term in relation (1).

As the repeated collisions inside the nuclei (an average of $\sim$3 collisions in emulsion nuclei) may give rise to a degradation of the Lorentz factor, the η variable could be defined using an average γ_c-value. However it must be noted that in the hundred-GeV range of energies the Lorentz factors of the secondary collisions are not too different from the first one, and then cannot shift the η-scale in such a way that the maximum value of R is reach for $\eta = 0$.

For these reasons we can exclude that the asymmetry in our correlation data can be due to a mere kinematical effect. ~~On the other hand~~ Moreover proton-neutron collisions cannot ~~justify~~ explain, alone, the results.

When looking at the results of the whole sample, including all N_h values (fig. 3 and 4) the correlations appear considerably high and the R-contours generally broader than in the different subsamples. As each N_h group contains interactions from different nuclei and with different multiplicities this fact suggests some caution when analysing the numerical results. The correlation function of a sample does not need to be just the mean of the subsamples [9,10], depending in a rather difficult way on η_1, η_2 and multiplicities. For these reasons our data have been also analysed using correlation functions different from $R(\eta_1, \eta_2)$ such as the widely used $C(\eta_1, \eta_2)$, $C'(\eta_1, \eta_2)$ etc.: nevertheless the asymmetry for $\eta_1 = -\eta_2$ always appeared clearly.

The same analysis performed on 200 GeV interactions, whose angular measurements we published elsewhere [11], has shown the same asymmetry effect.

The interpretation of the results could be attempted in the frame of current multihadron production models in proton-nucleus interactions [2,3,12-18]. Several of them predict that after the first collision the hadronic matter propagate inside the nucleus giving rise to two lumps: the faster of them can interact again, as the slower escape the nucleus disintegrating into pions. The hard lump is predicted to reproduce itself after each collision, giving rise to new slow lumps, but maintaining practically the same energy content as that of the incident proton.

From this point of view no change should be observed in the projectile hemisphere even if there are reiterate collisions inside the nucleus, so that the correlation function should not depend, in this kinematical region, on the number of collisions. A comparison made in this rapidity region between results coming from different N_h groups, but even from the available p-p data[4,7] seems to confirm these predictions.

In the same context all the slow lumps are confined in a rapidity region which, though depending on the specific model, roughly corresponds to some negative η interval. This feature is also confirmed by our experimental distributions (fig. 1 and 2), which just show a particle excess in the backward hemisphere, that becomes higher as N_h increases, but always remains in the same rapidity region. It is worthwhile to notice that in Gottfried energy-flux-cascade model[3] the slow slice mean rapidity is very close to the η-value that gives the maximum of $R(\eta_1, \eta_2)$.

Therefore these slow lumps could be considered as responsible of the enhancement of the correlation in the backward hemisphere, though it is difficult to infer from anyone of these models the effect on the correlation values: no one of them, indeed, takes explicitly into account any clusterization phenomenon in the disintegration of the fireballs.

REFERENCES

1) A.S.Goldhaber, Phys.Rev. D7(1973) 765.

2) P.M.Fishbane and J.S.Trefil, Phys.Lett. 51B (1974) 139.

3) K.Gottfried, CERN/TH-1735 (1973); Phys.Rev.Lett. 32 (1974) 957.

4) R.Singer et al., Phys.Lett. 49B (1974) 481.

5) J.Erwin et al., Phys.Rev.Lett. 33 (1974) 1443.

6) H.Dibon et al., Phys.Lett. 44B (1973) 313.

7) S.R.Amendolia et al., Phys.Lett. 48B (1974) 359.

8) Barcelona-Batavia-Belgrade-Bucharest-Lund-Lyons-Montreal-Nancy-Ottawa- Paris - Rome - Strasbourg- Valencia Collaboration, to be published.

9) A.Białas, K.Fiałkowski and K.Zalewski, Nucl.Phys. B48 (1972) 237.

10) P.Pirilä and S.Pokorski, Phys.Lett. 43B (1973) 502.

11) Barcelona-Batavia-Belgrade- Bucharest - Lund - Lyons - Montreal-Nancy-Ottawa-Paris-Rome-Strabourg-Valencia Collaboration, Phys. Lett. 48B (1974) 467.

12) A.Dar and J.Vary, Phys.Rev. D6 (1972) 2412.

13) P.M.Fishbane and J.S.Trefil, Phys.Rev.Lett. 31 (1973) 734.

14) A.S.Goldhaber, Phys.Rev.Lett. 33 (1974) 47.

15) G.Calucci, R.Jengo and A.Pignotti, Phys.Rev. D10 (1974) 1468.

16) A.Białas and W.Czyż, Phys.Lett. 51B (1974) 179

17) E.M.Friedländer, Nuovo Cimento Lett. 9 (1974) 349.

18) B.Anderson and I.Otterlund, Lund Preprint LUIP-CR-74-15 (1974); LUIP-CR-75-01. (1975).

Fig. 1 – Single particle inclusive distributions for three N_h (the number of heavy prongs) classes as a function of rapidity in c.m. (η) and laboratory (η_L) systems.

Fig. 2 – Two-particle inclusive distributions in c.m. backward (left) and forward (right) hemispheres for three N_h classes as a function of single particle rapidities.

Fig. 3 – Contour plots of the correlation function $R(\eta_1, \eta_2)$ for three N_h classes and for the whole sample of events.

Fig. 4 – Correlation function $R(\eta_1, \eta_2)$, for different N_h classes, as a function of rapidity separation $\eta_2 - \eta_1$ for different values of η_1. ● $\eta_1 = -2 \pm .75$, ■ $\eta_1 = 0 \pm .75$, ▲ $\eta_1 = 2 \pm .75$.

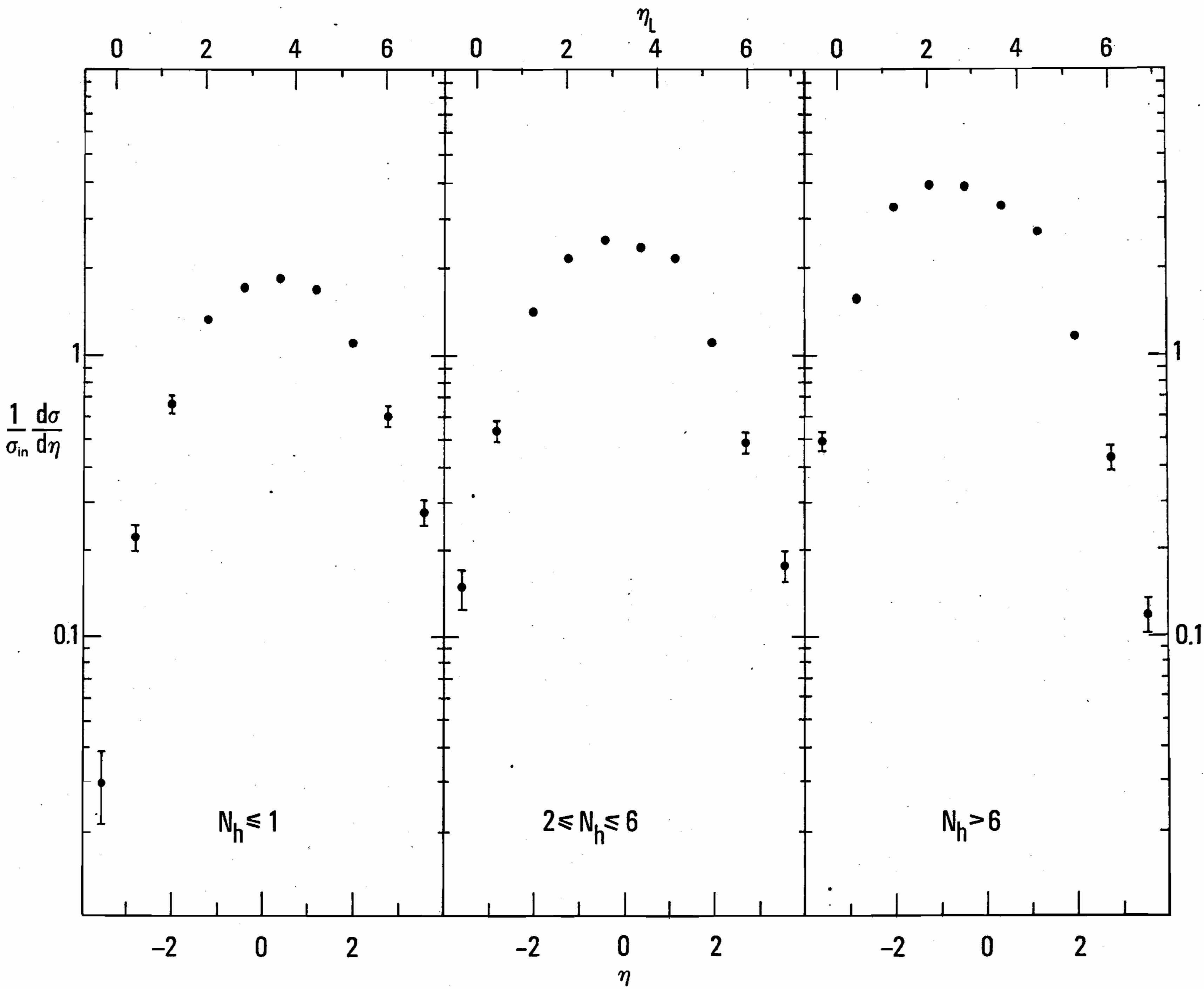
η_L
0
2
4
6
1
0.1
$\frac{1}{\sigma_{in}} \frac{d\sigma}{d\eta}$
$N_h \leq 1$
$2 \leq N_h \leq 6$
$N_h > 6$
-2
0
2
η

Fig 1

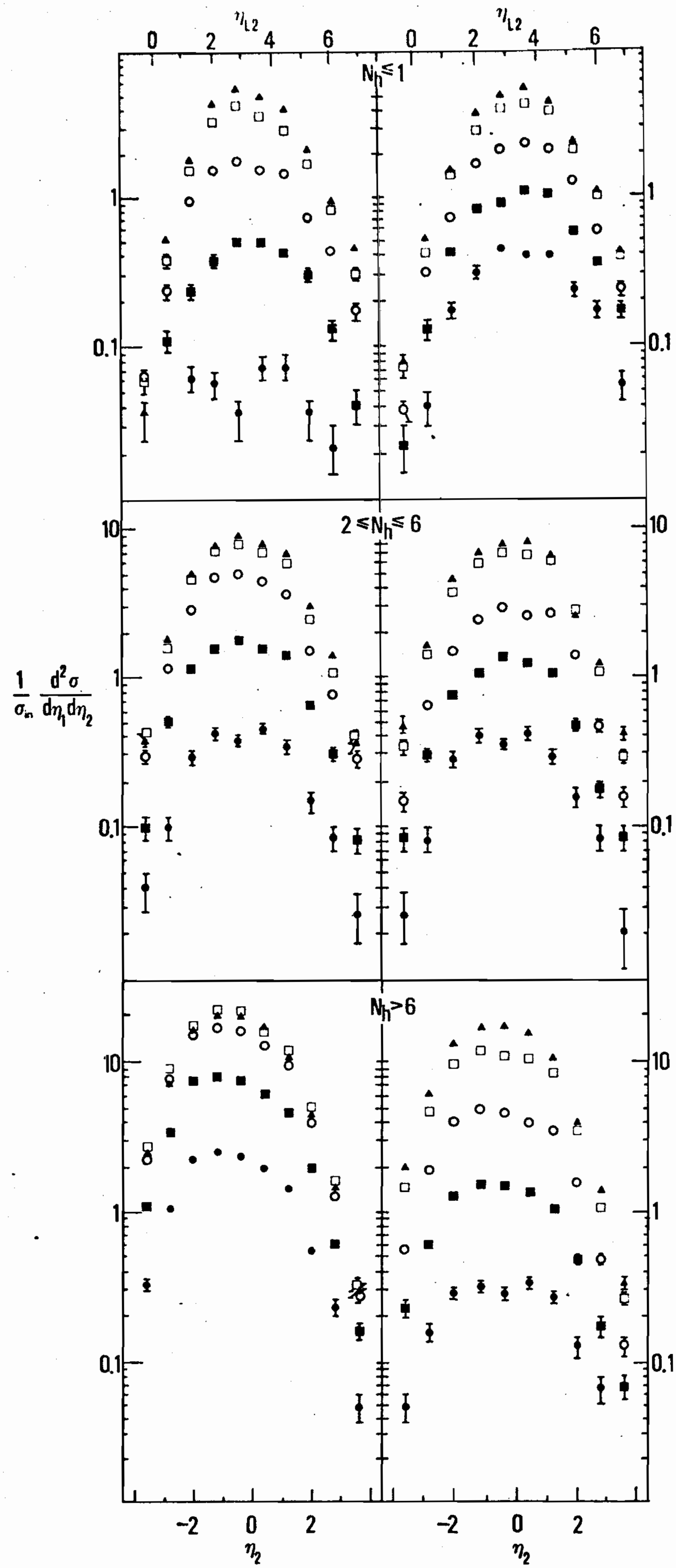

$-0.8 < \eta_1 < 0$ ▲ $0.0 < \eta_1 < 0.8$

$-1.6 < \eta_1 < -0.8$ □ $0.8 < \eta_1 < 1.6$

$-2.4 < \eta_1 < -1.6$ ○ $1.6 < \eta_1 < 2.4$

$-3.2 < \eta_1 < -2.4$ ■ $2.4 < \eta_1 < 3.2$

$-4.0 < \eta_1 < -3.2$ ● $3.2 < \eta_1 < 4.0$

Fig. 2

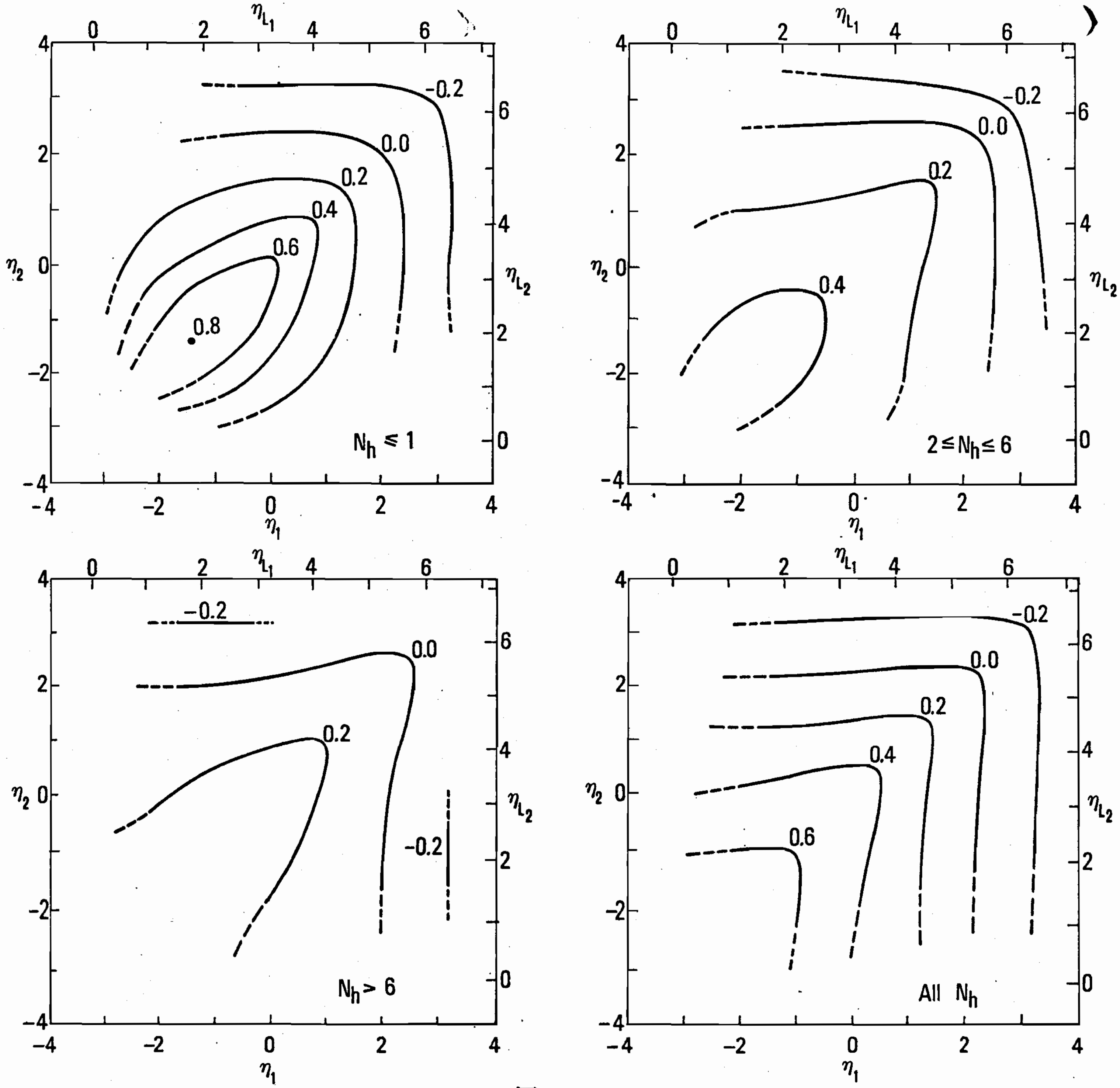

η_{L_1}
η_{L_2}
η_1
η_2
-0.2
0.0
0.2
0.4
0.6
0.8
$N_h \leq 1$
$2 \leq N_h \leq 6$
$N_h > 6$
All N_h

Fig. 3

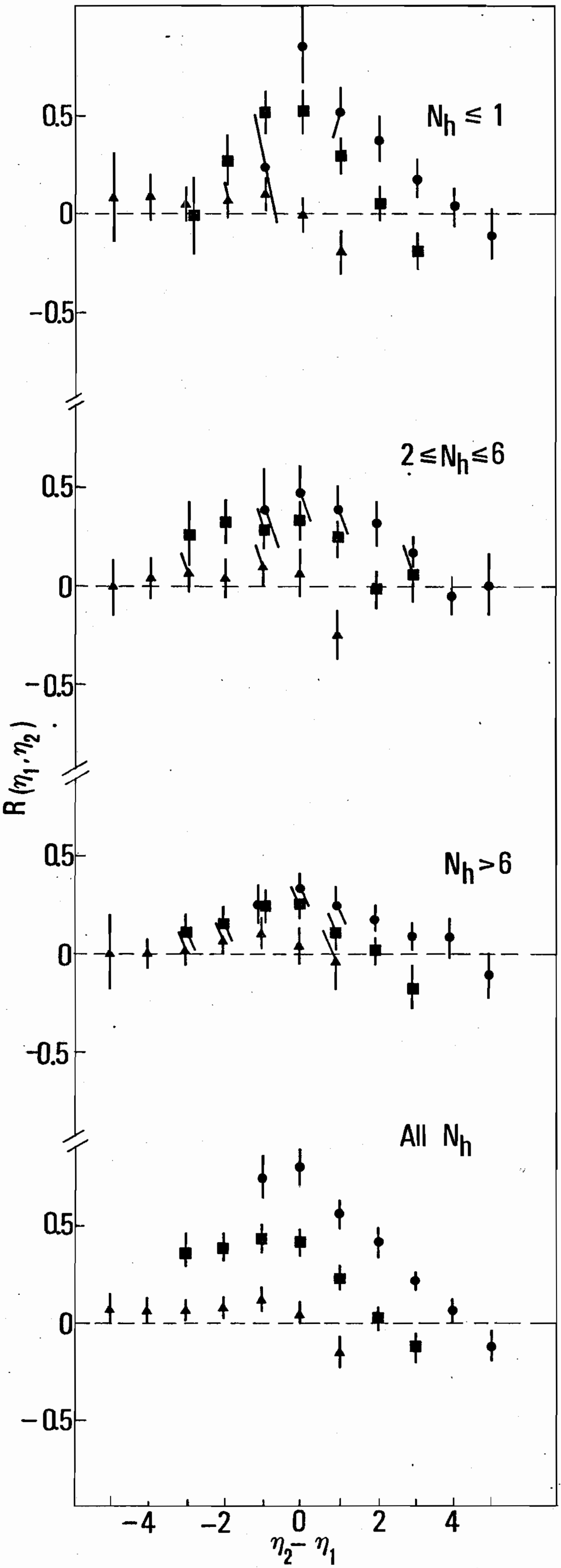

$N_h \leq 1$
$2 \leq N_h \leq 6$
$N_h > 6$
All N_h
0.5
0
−0.5
$R(\eta_1, \eta_2)$
−4
−2
0
2
4
$\eta_2 - \eta_1$